



Available online at [www.sciencedirect.com](http://www.sciencedirect.com)



Journal of Hydrology 283 (2003) 19–40

Journal  
of  
**Hydrology**

[www.elsevier.com/locate/jhydrol](http://www.elsevier.com/locate/jhydrol)

# Hydrogeological interpretation and potential of the new magnetic resonance sounding (MRS) method

M. Lubczynski<sup>a,\*</sup>, J. Roy<sup>b</sup>

<sup>a</sup>*Department of Water Resources (spec. Hydrogeology), ITC (International Institute for Geo-Information Science and Earth Observation), P.O. Box, 7500 AA Enschede, The Netherlands*

<sup>b</sup>*Department of Earth System Analysis (spec. Geophysics), ITC (International Institute for Geo-Information Science and Earth Observation), P.O. Box, 7500 AA Enschede, The Netherlands*

Received 21 August 2002; accepted 23 April 2003

## Abstract

This study reviews the up-to-date hydrogeological contribution of the new, geophysical magnetic resonance sounding (MRS) method and presents new interpretation ideas and potential regarding various hydrogeological applications. The main advantage of the MRS method as compared to other geophysical methods is in its water selectivity. MRS is commercially available but is also the subject of R & D to minimize a number of limitations related not only to data acquisition but also to hydrogeological data interpretation. The two main MRS output data types are free water content ( $\Phi_{\text{MRS}}$ ) and decay time constant ( $T_d$ ). Relations between  $\Phi_{\text{MRS}}$  and effective porosity, specific yield and specific storage are discussed in the framework of an original groundwater storage concept.  $T_d$  is correlated empirically with hydraulic conductivity, however such correlation is not yet quantified for various rock types so  $T_d$  has to be calibrated by borehole data. As an improvement of the data interpretation, a proposal of a new, multi-decay approach is presented. The advantage of such analysis is that it combines storage and flow property characteristics in assessing water content at various pore size fractions, and the disadvantage is that it is applicable only at large signal to noise ratios. Five case examples are used to show that combined interpretation of  $\Phi_{\text{MRS}}$  and  $T_d$  can be used to evaluate subsurface hydrostratigraphy although such analysis is vulnerable to equivalence error and its resolution decreases with depth. MRS with large volume-averaging schema and current limitation to 1D approach is already suitable for groundwater modelling applications and for evaluation of groundwater potential in the MRS measurement scale ( $\sim 100 \times 100 \text{ m}^2$ ) but is not yet optimized for well siting. MRS can detect water in the unsaturated zone, which can be potentially used in real time subsurface flux monitoring. Field experiments indicate that MRS is not appropriate for groundwater salinity detection. No field experiments have yet been made to detect hydrogenated compounds like hydrocarbons and tracers in the subsurface.

© 2003 Elsevier B.V. All rights reserved.

**Keywords:** Magnetic resonance sounding; Hydrogeological interpretation; Aquifer storage; Hydraulic conductivity; Groundwater potential

## 1. Introduction

Various methods of subsurface investigation are known in hydrogeology. They are either invasive like those where physical subsurface penetration is needed

\* Corresponding author.

E-mail addresses: [lubczynski@itc.nl](mailto:lubczynski@itc.nl) (M. Lubczynski), [roy@itc.nl](mailto:roy@itc.nl) (J. Roy).

(investigation boreholes including borehole logs, pumping and tracer tests, standard soil moisture or suction pressure profiling etc.) or noninvasive like surface electrical and electromagnetic methods, ground penetrating radar methods etc. Invasive methods are expensive and time consuming while surface noninvasive geophysical methods are largely non-unique with respect to the discrimination between water and medium. A new, hydro-geophysical method magnetic resonance sounding (MRS) has a great future due to the applied nuclear magnetic resonance (NMR) principle well described in the context of borehole logging applications e.g. in Allen et al. (1997). In the MRS technique, an excitation is made from the ground surface

(non-invasive sounding) with the MRS instrument at the Larmor (resonance) frequency  $f = 0.04258 \cdot B$ , predetermined with a standard magnetometer by measuring the earth's magnetic field ( $B$ ). Currently there is only one MRS instrument commercially available called NUMIS<sup>PLUS</sup> (an other one called HYDROSCOPE is available only in Russia) as presented in Fig. 1 (IRIS Instruments, 2002). The NUMIS instrument consists of the following equipment units (numbers as in Fig. 1): (1) two identical DC/DC converters used to program a variable amount of electric energy to produce the loop excitation current in a form of required pulse moment ( $Q$ ); (2) the main MRS unit used both for the AC loop excitation and the signal acquisition; (3) a reel of copper cable

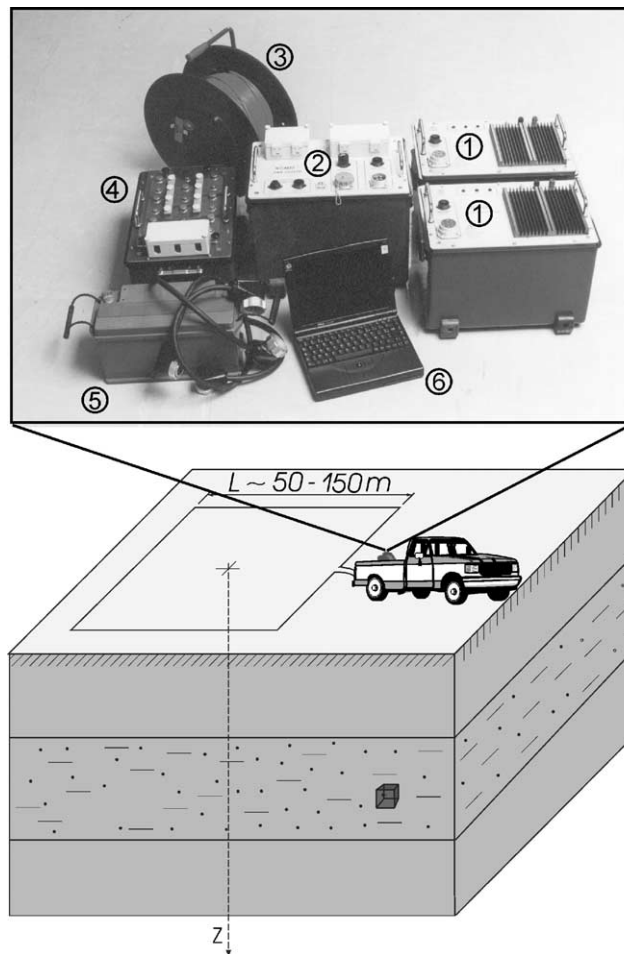


Fig. 1. Commercial MRS equipment: NUMIS<sup>PLUS</sup> (IRIS Instruments, 2002).

used to layout the loop usually laid down as a square, AC current loop of 50–150 m length of the side (Fig. 1); (4) a tuning box; (5) a high capacity rechargeable battery used to power the system and (6) a normal PC laptop for overall system control, data recording and processing. In MRS technology instead of a laboratory-generated magnetic field, the earth natural magnetic field is used as a static field. Upon termination of the excitation, an in-situ hydrogen nuclei precession continues freely for a short time, usually less than one second, generating a weak NMR AC magnetic field detectable at the surface. The complete MRS field sounding is composed of a number of measurements, whereby the investigated volume is energized with systematically increased excitation pulse moments  $Q = I \cdot \tau$  ( $I$  – current [A],  $\tau$  – excitation time [ms]) generated by the MRS instrument at the Larmor frequency. From the series of such excitations, the initial signal amplitude  $E_0$  versus  $Q$  is made as shown in Fig. 2a. In Fig. 2b an

excitation current in a single excitation is shown, followed by a 30 ms ‘dead-time’ (time between the termination of the excitation and first signal measurement) during which no measurement can be made. Next in Fig. 2c, the decaying signal recorded in time ( $t$ ) is presented. The envelope of this signal is usually modelled by the following equation:

$$E(t) = E_0 \exp(-t/T_d) \cos(2\pi ft + \varphi) \quad (1)$$

where  $E_0$  is the initial signal amplitude derived from the NMR signal decay envelope (Fig. 2c),  $T_d$  decay time constant and  $\varphi$  phase shift between the signal and excitation current are the three parameters extracted from the signal. The inversion of  $E_0$  and of  $T_d$  as a function of  $Q$  yields two types of hydrogeologically significant information: free water content ( $\Phi_{MRS}$ ) and decay time constant ( $T_d$ ) both as a function of depth. In the standard inversion tool  $\varphi$  is not used. It provides, however, data acquisition quality control.

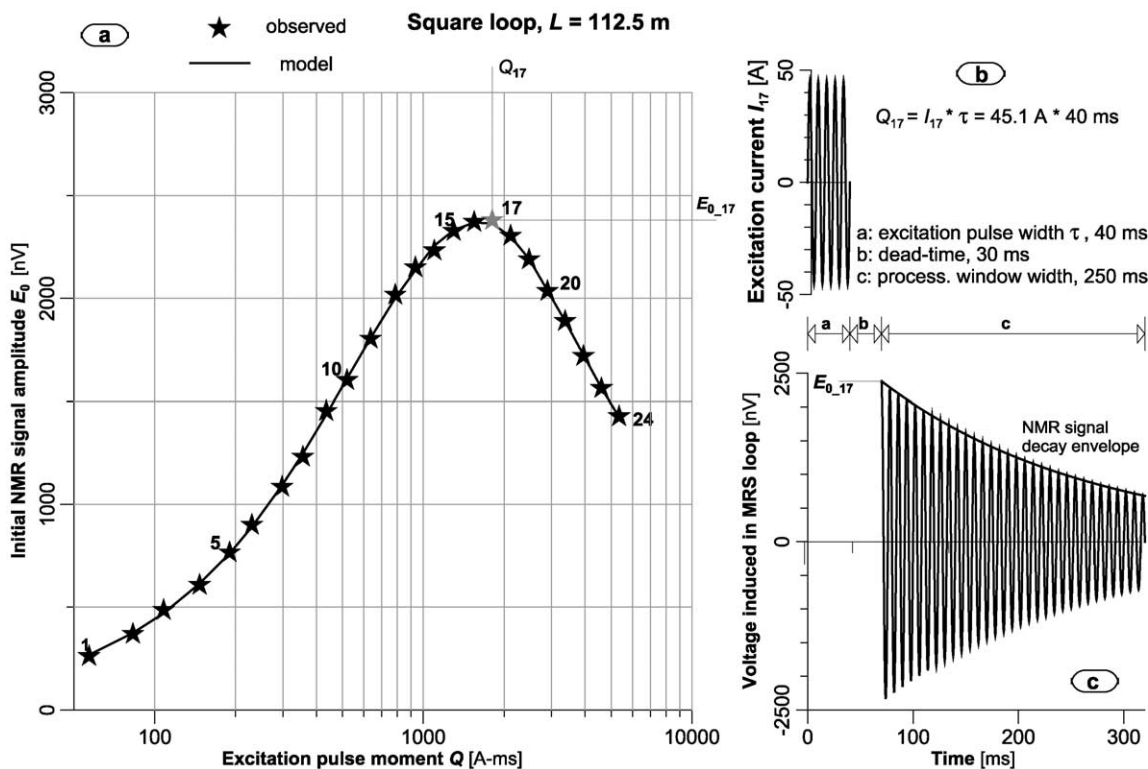


Fig. 2. MRS data acquisition at site Waalwijk-2 (The Netherlands): (a) sounding summary:  $E_0$  vs.  $Q$ ; (b) excitation pulse moment; (c) voltage induced in the MRS loop by the  $^1\text{H}$  precessing nuclei. (Frequency scaled down by 16 for display purpose).

The main advantage of MRS as compared to other classical geophysical methods is that it is water selective, which means that an excitation is at the specific hydrogen nuclei resonance precession frequency so the response is unique for water (e.g. groundwater). Techniques such as resistivity methods or time domain electromagnetic (TDEM) lack this feature. The MRS technique is still undergoing development. The most important limitations are related to MRS investigations in electrically conductive environments, in environments with low S/N (Signal to Noise) ratio and in areas with inhomogeneous magnetic field. In electrically conductive environments, an inversion is distorted by attenuation of a signal by conductive layers. This limitation can be improved, up to the certain degree, by application of a resistivity model, which, however, requires separate use of an electrical and/or electromagnetic method next to MRS, [Shushakov \(1996\)](#) and [Legchenko and Shushakov \(1998\)](#). The acquisition of a valid MRS data set is also substantially dependent on the S/N ratio. The NMR signal is dependent not only on the in-situ groundwater content and its depth, but also on the strength of the earth's spatially dependent magnetic field, whereas the noise is related to lightning and/or artificial man-made noise sources i.e. electrical power lines etc. At locations characterized by very low S/N ratios ( $S/N \ll 1$ ), the acquisition of a valid MRS data set is not practical because it is either too long or it is not possible at all. There are also some locations where even the shallow-lying productive aquifers cannot be detected with current MRS instrumentation because of inhomogeneous magnetic field. Other important MRS limitations in hydrogeological applications are: (1) restricted to 1D data acquisition and inversion; (2) even in favorable S/N ratio and electrically resistive conditions the penetration depth is still instrumentally limited to  $\sim 100$  m due to the combined limitations on loop size and maximum  $Q$  (excitation pulse moment); (3) the  $T_d$  measurement is limited by dead-time of 30 ms and in practice is restricted to  $T_2^*$  while an apparent  $T_1$  can now be estimated (see explanation below). A more complete description of the MRS technique itself can be found in [Goldman et al. \(1994\)](#), [Roy and Lubczynski, \(2000a\)](#), [Legchenko et al. \(2002\)](#),

[Roy and Lubczynski \(2003\)](#) and [Lubczynski and Roy \(2004\)](#).

This MRS assessment is based on experience with NUMIS MRS technology evaluated in the period up to the end of 2001.

## 2. Literature overview

Since the origin of the MRS method till the late '80 s, the MRS technique was known only to a restricted Russian group from Novosibirsk. The first Russian MRS instrument called HYDROSCOPE was extensively used at that time in Russia, mainly in Siberia where a strong magnetic field is favorable for a good S/N ratio and thus for MRS measurements ([Lubczynski and Roy, 2004, Fig. 6](#)). Unfortunately very little material is available from those experiments. Since the beginning of the 90s when MRS and HYDROSCOPE became more widely known, particularly in the middle 90s when the French instrument NUMIS came on the market, a rapid MRS technology development started. Since then, the hydrogeological verification was intensified, before 1998 in a rather qualitative manner and since 1998 in a more quantitative manner as described below.

In the period before 1998, the comparison of the  $\Phi_{\text{MRS}}$  with borehole logs and/or results of other geophysical methods is presented by various researchers e.g. [Semenov \(1987\)](#), [Schirov et al. \(1991\)](#), [Goldman et al. \(1994\)](#), [Trushkin et al. \(1994\)](#), [Trushkin et al. \(1995\)](#), [Gev et al. \(1996\)](#) and [Shushakov \(1996\)](#). The most systematic comparative analysis of  $\Phi_{\text{MRS}}$  and related lithological grain volume fractions, is provided by [Lieblich et al. \(1994\)](#) although the reported MRS tests were made at sites apparently unfavorable for a 1D technique. It is also interesting to note the HYDROSCOPE calibration test performed on the Ob river ([Schirov et al., 1991](#)), where 100% of  $\Phi_{\text{MRS}}$  for the water body below a thin ice cover was obtained by HYDROSCOPE inversion. Unfortunately, the complete quantitative description of this experiment is not available. The first hydrogeological interpretation of the HYDROSCOPE  $T_2^*$  in terms of transmissivity ( $T$ ) is mentioned in [Schirov et al. \(1991\)](#). In [Goldman et al. \(1994\)](#), it is explained how  $T$  is obtained using HYDROSCOPE  $T_2^*$  inversion although

the explanation on how  $T_2^*$  is transformed into  $T$  is not available. An attempt was made to compare MRS originated  $T$  with pumping test  $T$  (not quoted by the authors). A discrepancy in a range of 2–3 orders of magnitude was obtained which resulted in the final statement that ‘transmissivity and pore size, these are parameters less reliably determined’. Later no more HYDROSCOPE  $T$  interpretation was published (in Western literature). Concerning MRS performance in saline water environments Goldman et al. (1994) concluded that MRS is not a salinity-measuring tool although its integrated use with TDEM enhances the reliability of TDEM application in salinity estimates (Goldman et al., 1994; Trushkin et al., 1995; Shushakov, 1996).

In the period since 1998 more quantitative MRS studies have been carried out with hydrogeological cross validation. In 1998, at the Environmental and Engineering Geophysics Society (EEGS) meeting in Barcelona, Legchenko et al. (1998) presented a linear correlation between signal amplitude and borehole pumping rate for a number of wells tested and Roy et al. (1998) verified MRS using a slug test and core recovery log from a well bored after the MRS measurement had been done. Verification of the MRS water content by core sampling combined with geophysical logging is presented by Yaramanci et al., (1999). Verification of the MRS extractable groundwater water content using pumping test data (single well tests) on a Southern African Karoo Sandstone layer is presented by Roy and Lubczynski (2000b) and Kgotlhang (2000). Verification of Seever’s and Kenyon’s formula for calculation of hydraulic conductivity and correlation of MRS transmissivities with transmissivities obtained from well pumping tests is presented by Legchenko et al. (2002) in the special, MRS dedicated issue of the Journal of Applied Geophysics from May 2002 where a number of hydrogeologically focused MRS papers have been published. The complete hydrogeological and geophysical review of MRS capabilities and limitations is presented in Lubczynski and Roy (2004).

### 3. Aquifer parameterisation

MRS technology and its capability for hydrogeological aquifer parameterization is discussed on

the base of the sounding example Waalwijk-2 (Figs. 2 and 3) from The Netherlands presented next to other four sounding results from Botswana (2), France and Portugal. The site Waalwijk-2 with a high S/N = 96 was selected for more detailed MRS interpretation, to avoid noise-induced indeterminations in MRS data interpretation. Such a high S/N ratio was attributed to the strong signal due to the water abundant multi-layered aquifer system and low artificial noise (nature park location) as well as low natural noise at the time the sounding was made. The other four presented sounding results had the following S/N ratios: Serowe (Botswana) – 0.8, Palla Road (Botswana) – 1.6, St. Cyr en Val (France) – 8.3 and Lameira (Portugal) – 4.0. The hydrogeological schematization of the five MRS test sites is discussed hereafter and presented down to 100 m depth in Fig. 3a.

The Waalwijk-2 MRS site is located at 51°39′09″N and 5°06′57″E ( $X = 136225$  and  $Y = 407100$  in the local Dutch Rijksdriehoeksmeting coordinate system). The hydrogeological log representative for that site has been estimated from the nearby (<3 km), abundant boreholes, hydrogeological expertise with pumping test data and numerical models (TNO, 2002). The subsurface lithology at the Waalwijk-2 test site location can be characterized as a three layer multi-aquifer system (only two aquifers shown in Fig. 3a) separated by clay-rich layers (aquitards) in which downward leakage occurs (head decline with depth reported). The upper unconfined (static groundwater table ~6 m b.g.s), 46 m thick and highly permeable aquifer (horizontal hydraulic conductivity  $K_h = 24$  m/d), which is the main target of the Waalwijk-2 MRS test, is comprised of the Nuenen Subgroup and Sterksel Formation. The underlying 33 m thick clay aquitard (vertical hydraulic conductivity  $K_v = 0.004$  m/d) is intercalated with sandy deposits. The second aquifer ( $K_h = 5$  m/d) is separated from the third aquifer ( $K_h = 15$  m/d) by relatively thin, 5 m clay aquitard characterized by  $K_v = 0.015$  m/d. All the above-specified  $K$  values of the schematized layers, aquifers and aquitards, are extracted from the REGIS database (TNO, 2002). With regard to storage property evaluation, only the estimate of the Nuenen-Subgroup specific yield ( $S_y$ ) of 0.3 of the upper layer is available (TNO, 2002). For generic guidelines regarding the range of porosity, effective porosity and specific yield of

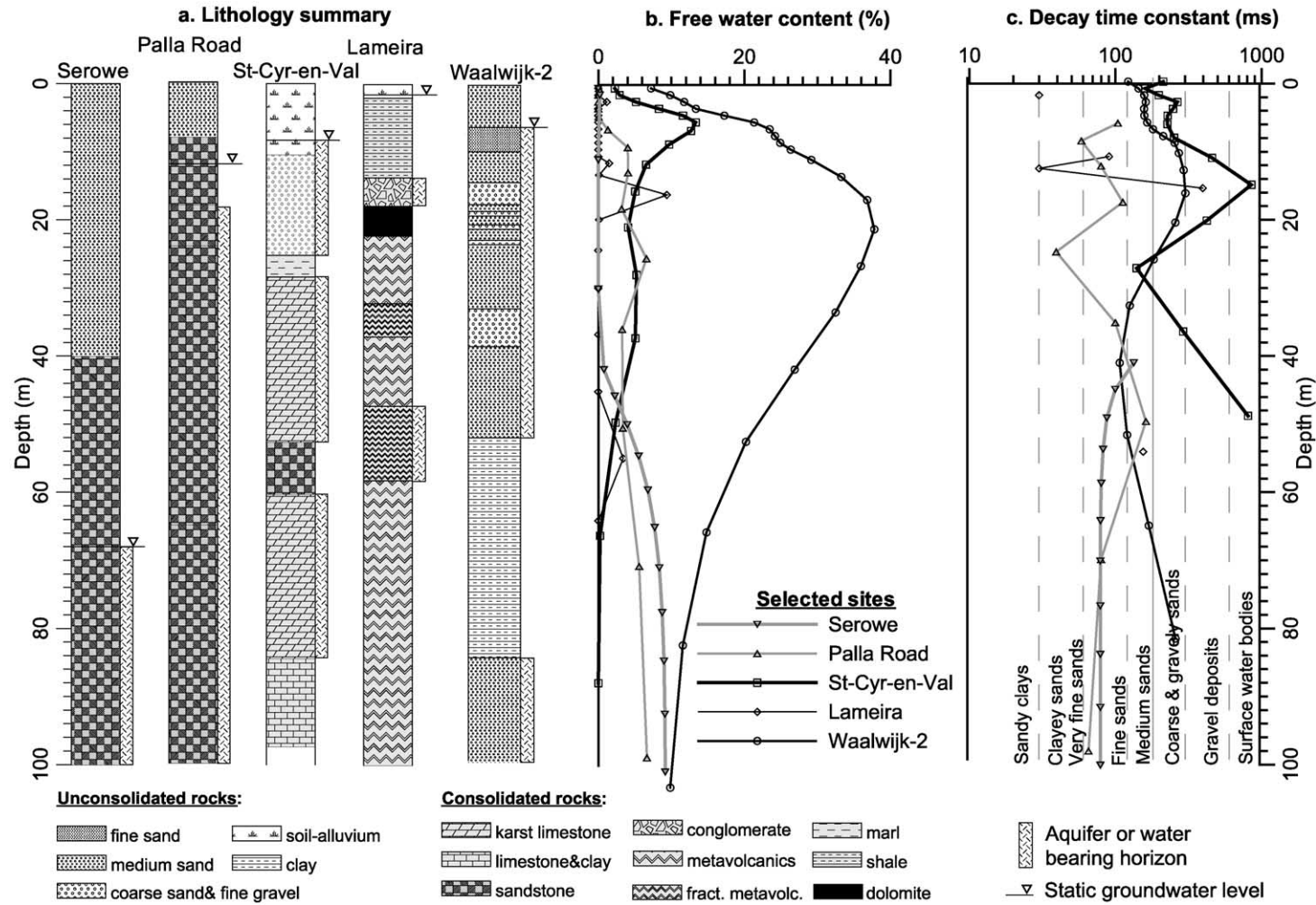


Fig. 3. MRS sounding example at five selected test sites (Serowe, Palla Road, St-Cyr-en-Val, Lameira and Waalwijk-2): (a) Hydrogeologically schematized subsurface; (b) MRS water content ( $\Phi_{MRS}$ ) with depth; (c) MRS signal decay time constant ( $T_2^*$ ) with depth including Schirov et al. (1991) decay relationships.

the unconsolidated deposits the reader is referred to (Rawls and Brakensiek, 1985; Maidment, 1993).

The Lameira (Portugal) MRS site (UTM Zone 29, 642255, 4216409) is located within the Moura-Ficalho carbonate fractured and karstic aquifer system (Fig. 3a). The MRS sounding was performed at ~1 km distance off the aquifer anticline core outcrop composed of Cambrian dolomites. Despite the quite close distance, the MRS test did not identify the target aquifer within the depth of 60 m b.g.s. After the MRS test, an investigation borehole was drilled down to 207 m to test the MRS findings (Roy et al., 1998). Under approximately 2 m thick soil and impermeable shales reaching down to 13.7 m b.g.s., a 5 m thick confined water bearing horizon of Tertiary conglomerates was found, for which  $T = 25 \text{ m}^2/\text{d}$  was estimated by slug testing. Within the underlying 115 m thick Ordovician impermeable metavolcanics sequence two fractured zones were identified, first at 32–37 m b.g.s. filled with clay and second at 48–58 m b.g.s. without clay. The target Cambrian dolomites, correspondent to the Moura-Ficalho aquifer were found at 133 m b.g.s. beyond the MRS access capability with no important water resources.

At the St-Cyr-en-Val site in France (UTM Zone 31, 422740, 5293026) MRS sounding was performed at the location with three distinct aquifers, which has been hydrogeologically investigated by BRGM (Legchenko et al., 1995). The upper unconfined aquifer (groundwater table at ~8.3 m b.g.s.) is composed of 10 m thick alluvial deposits and a 15 m thick layer of mixed gravel, sand and clay, both underlain by 3 m thick impermeable marl (Fig. 3a). Below there are two karstic limestone aquifers separated by a low permeable sandstone layer at 52–60 m b.g.s. The total thickness of all aquifers is around 70–80 m with an average porosity of 10% and a  $T = 0.28 \text{ m}^2/\text{s}$ , which leads to an estimate of  $K \cong 300 \text{ m/d}$ .

Two MRS soundings made at Serowe and Palla Road sites correspond to two national scale groundwater resources projects in Botswana. The Serowe sounding is located next to the borehole BH 5301 (UTM zone 35, 453500, 7536700) with  $22 \text{ m}^3/\text{h}$  borehole yield and Palla Road sounding next to the borehole BH 7583 (UTM zone 35, 476693, 7397144) with  $118 \text{ m}^3/\text{h}$  yield. Both locations have a comparable hydrogeological set-up, with unconsolidated Kalahari

Sand overlying the main Ntane Sandstone aquifer, in Serowe with a 40 m thick cover and in Palla Road with an 8 m cover. The Serowe sounding is located in the recharge area and the aquifer is unconfined with relatively low  $K \cong K_h = 1 \text{ m/d}$  and  $S_y = 0.04$ . The Palla Road sounding is located in the discharge area, at the highly fractured outlet of the hydrogeological Palla Road basin. The sandstone aquifer with locally extended leaky confined silty sandstone sections (the whole profile of silty sandstone was found to be wet at the time of drilling), has  $K > 10 \text{ m/d}$ , pumping test transmissivity  $T > 1000 \text{ m}^2/\text{d}$  and  $S_y = 0.02$ . All presented Botswana  $K$  and  $S$  values are extracted from the numerical models available for both areas analyzed (WCS, 1994, 2000).

### 3.1. Water content interpretation

In the MRS technique the subsurface water content is evaluated through the geophysical inversion of the  $E_0 = f(Q)$  curve (Fig. 2a) with instrument specific software NUMIS. As a result MRS free water content ( $\Phi_{\text{MRS}}$ ) is obtained as a function of depth (Fig. 3b). The important aspect is to translate this term into a commonly used water storage term. Regarding a soil/rock-water relationships related to the storage evaluation, there are differences between the disciplines of hydrology, soil science and geophysics, particularly with respect to the terminology of the least defined microscopic processes at the pore-water contact. Therefore to understand the meaning of the measured  $\Phi_{\text{MRS}}$ , the MRS subsurface water storage concept is presented below and illustrated in Fig. 4.

Free water content ( $\Phi_f$ ) is the percentage of water that is outside the field of molecular forces of attraction of the solid particles that can be displaced by gravity or pressure gradients, as compared to the total rock volume. Bound water ( $\theta_b$ ) in contrast to free water is the amount of water attached to the solids by molecular forces of attraction, non-removable by gravity and/or pressure gradient forces but removable by centrifugal action defined e.g. by Polubarinova-Kochina (1962) at acceleration 70,000 times exceeding the acceleration of gravity. Bound water surrounding a solid consists of two zones (Fig. 4) differing in forces of attraction to the solid, an internal zone of firmly bound water approximately  $0.1 \mu\text{m}$  thick, which can practically be treated as a solid due to

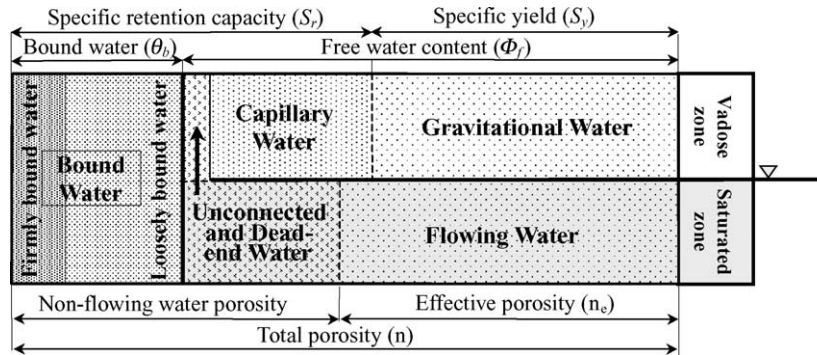


Fig. 4. Groundwater storage concept.

the very strong forces of attraction and an external transition zone of loosely bound water with arbitrarily defined water film thickness of  $\sim 0.1\text{--}0.5\ \mu\text{m}$  (Polubarinova-Kochina, 1962). The bound water film surrounding a solid varies with the grain size of the solids, their surface area and mineral type (Grabowska-Olszewska and Siergiejew, 1977; Coates et al., 1998). The thickness of the bound water film is influenced by the strength of the forces of attraction and is correlated with the MRS signal decay time ( $T_d$ ), although the exact relation is not known. So far in the NMR studies (Timur, 1969; Coates et al., 1998) and in MRS studies as well (Schirov et al., 1991; Goldman et al., 1994; Lieblisch et al., 1994) it is assumed that the measured signals after the 30 ms dead-time (current instrumental characteristic), have a decay rate corresponding to free water ( $\Phi_{\text{MRS}} \cong \Phi_f$ ). Although signals with a decay rate slightly faster than 30 ms can be detected, it is widely and arbitrarily assumed (also in the continuation of this paper) that with the available instrumentation only free water is measured. This aspect however, requires further investigation as well as MRS relation between the decay rate and the size of the bound water film on the various rocks and minerals.

In the saturated zone (displayed in the lower part of Fig. 4), the free water content ( $\Phi_f$ ) consists of the effective porosity (fraction of the rock occupied by the water free to flow) and unconnected and dead-end pores as defined by Marsily (1986). Effective porosity ( $n_e$ ) defined as a proportion between Darcian velocity and true linear velocity of groundwater flow is a kinematical parameter often applied in aquifer flow and transport modelling. In microscopic processes it

refers to the continual exchange of molecules from one phase to the other through molecular Brownian motion. For example, a circulating molecule may become immobilized in the course of its progress, while another one that was originally immobile may be set in motion (Marsily, 1986). Dead-end porosity (fractures and micro-joints but also non-flowing karstic cavities etc.) often plays an important role in karstic and hard rocks while unconnected pores are abundant in volcanic and karstic rocks. In unconsolidated sediments the role of unconnected and dead-end porosity is negligible or can even be disregarded as is suggested by Fetter (1994, p. 81). If the MRS sounding is performed over the rocks where the dead-end and unconnected porosity can be neglected,  $\Phi_f$  and therefore  $\Phi_{\text{MRS}}$  as well, can be directly interpreted as  $n_e$ .

Many groundwater applications are related to well abstractions. If an unconfined aquifer is desaturated by well abstraction, the quantity of gravitational water (water that can be released by gravity forces) is determined by specific yield ( $S_y$ ). The remaining water in the desaturated part of an aquifer represents the total unsaturated specific retention capacity ( $S_r$ ), in soil science known as moisture at field capacity ( $\theta_{\text{FC}}$ ), which consists of bound water ( $\theta_b$ ) and a portion of free water retained against gravity forces ( $\theta_f$ ). The latter can be of the following origin: (1) water of unconnected porosity (usually minimal contribution) – if pores are sufficiently large ( $T_d > 30\ \text{ms}$ ) then such water is ‘seen’ by MRS (e.g. in volcanic and karstic rocks); (2) water of the dead-end pores not allowing for gravity water release – this is an important contribution only in secondary porosity rocks; (3) free capillary water ( $\theta_c$ )—usually the main



$\theta_f$  contribution in the unsaturated zone, represents part of the free water resistant to gravity release and driven by hydraulic head difference (but not gravity), which after rock desaturation ‘wets’ the solids (air stays in the middle of the voids) surrounding them with capillary water attached to the solids by surface tension forces.

Under the assumption of  $\Phi_{MRS} \cong \Phi_f$ ,  $S_y$  can be calculated from  $S_y = \Phi_{MRS} - \theta_f$ . Practical definition of  $\theta_f$  is cumbersome, so instead use of  $S_r$ , is more convenient although only if  $\theta_b$  can be neglected. By applying  $S_r$  instead of  $\theta_f$  it is expected that the  $\Phi_{MRS}$  measurement provides the entire spectrum of water content including bound water, which in practice is not the case yet because current instrumental limitations do not allow for measurement of a signal  $< 30$  ms. As soon as this limitation is overcome, the  $S_y$  can be properly estimated from  $S_y = \Phi_{MRS} - S_r$  where  $S_r$  can either be arbitrarily estimated as shown in Fig. 5 or through the estimate of  $\theta_{FC}$  by other known hydrological methods (Maidment, 1993). Practical water supplying applications however focus on water bearing

aquifers normally composed of coarse rock materials allowing for the assumption  $\theta_f \cong S_r = \theta_{FC}$  which permits only slight underestimation in  $S_y$  estimate (by the amount of bound-water included in  $\theta_{FC}$ ).

In confined aquifers, elastic water release is not related to the gravity dewatering process, as is the case in unconfined aquifers, but to the water expansion and aquifer compaction effect attributed to aquifer pressure changes. If the aquifer compressibility ( $\alpha$ ) and water compressibility ( $\beta$ ) can be estimated, the specific storage ( $S_s$ ) value depends then upon the porosity ( $n$ ) value according to the formula  $S_s = \rho g(\alpha + n\beta)$  where  $\rho$  is water density and  $g$  is gravity acceleration. Currently,  $n$  is underestimated by the instrumentally limited estimate of  $\Phi_{MRS}$  neglecting bound water. The overall storage term is then calculated from the formula  $S = D \cdot S_s$ , where  $D$  is a layer thickness, which also can be estimated by MRS (see section Aquifer Geometry).

In the geophysical inversion  $\Phi_{MRS}$  is determined at certain depth intervals; the larger the  $h/L$  ratio ( $h$  : depth,  $L$  : loop size), the larger the influence of

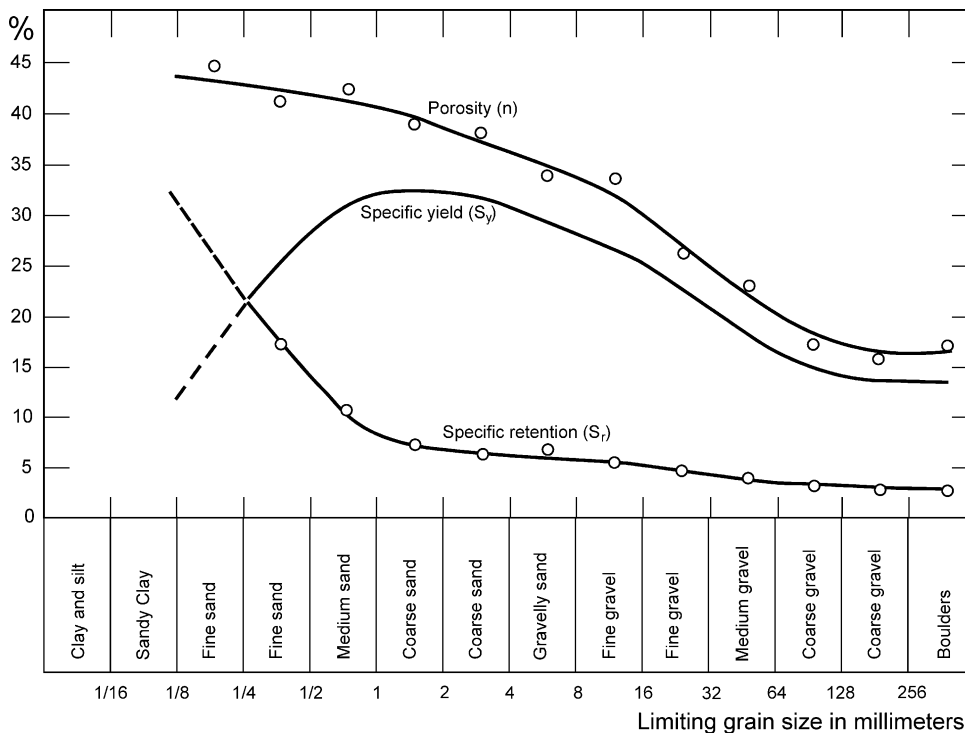


Fig. 5. Relation between specific yield and retention capacity (redrawn after Todd (1959)).

equivalence error in the inversion results. A more reliable quantitative interpretation of water content at certain analyzed depth intervals, can be done by integrating the product of  $\Phi_{\text{MRS}} \cdot D = H_w \cong \Phi_f \cdot D$  (Legchenko and Shushakov, 1998) with depth, where  $H_w$  is a free hydrostatic column of water.  $H_w$  can be estimated for single layers of interest like aquifers but also for the arbitrary depth intervals like e.g.  $H_{\text{wm}}$  estimated for the maximal MRS investigation depth.

An example of  $\Phi_{\text{MRS}}$  inversion for the five sites described earlier is presented in Fig. 3b. The figure is built with a commonly used scheme of pre-setting the number of depth intervals equal to the number of  $Q$  values used to perform the MRS survey. At Waalwijk-2 this number was equal to 24 but often, as in the other cases presented (Fig. 3), a number of 16 is used. The maximum depth at which these depth intervals are determined, is selected by the operator taking into account the loop shape, the loop size, the maximum  $Q$  value and the subsurface electrical conductivity.

In Waalwijk (Fig. 3b), the first interpreted layer is an unsaturated zone 0–6 m where  $\Phi_{\text{MRS}}$  rapidly increases from about 7% at the surface to  $\Phi_{\text{MRS}} = 22\%$  at 6 m b.g.s. Substantially variable  $\Phi_{\text{MRS}}$  with depth is likely to result from the occurrence of retained water in the capillary fringe. At approximately 6 m b.g.s. at the groundwater table level, a distinct break point in the  $\Phi_{\text{MRS}}$  is observed. Below this, the variation of  $\Phi_{\text{MRS}}$  with depth is likely to be attributed to lithological and granulometric differences with depth. At the depth interval of 6–10 m, corresponding to a fine sand layer, the  $\Phi_{\text{MRS}}$  slope is reduced. Below this,  $\Phi_{\text{MRS}}$  increases in medium to coarse sand interval between 10 and 14.5 m and continues increasing downward where the gravel layer starts. This gravel layer continues down to 17.5 m b.g.s. and the section below, down to 21.5 m, is composed of interchanging thin layers of coarse sand and fine gravel. From 21.5 m down to 52 m b.g.s. a medium sand is dominant although some ~1 m thin layers of fine sand and a single thick gravel layer at 33–39 m b.g.s. are present. At 52 m b.g.s. the clayey aquitard starts, which is composed of sandy clay at upper 10 m and pure clay down to 85 m b.g.s. Clay normally contains a higher percentage of water than sand or gravel, however the pore size of the clay is much smaller, which implies that the majority of water is stored in pores too small to be detected with

instrumental dead time (30 ms). This is reflected by a substantial drop of  $\Phi_{\text{MRS}}$  with depth, which represents measurable water only. Below 85 m where the second aquifer starts, an expected increase of  $\Phi_{\text{MRS}}$  is not observed. Taking into account the resistivity profile established on the available borehole logs, the numerical modelling shows that with the survey parameters used (loop size, loop shape and range of excitation moment used), it is not possible to discriminate responses between the first aquifer, clay aquitard and second aquifer using standard MRS inversion tools. It is an example of the loss of resolution with depth. The Waalwijk-2 site has the highest free water storage capacity as compared to other four sites evaluated and that is reflected by high  $H_{\text{wm}} = 22.4$  m estimated for the interval of 100 m b.g.s.

In Lameira, shallow free water is detected near the surface (<2%) at ~3 m b.g.s. (Fig. 3a and b) in the soil and unconsolidated deposits. It is a thin water film of the recent rain recharge accumulated at the top of the underlying low permeable shale layer. The conglomerate layer at ~14–18 m b.g.s., is the most porous horizon identified by the increase of  $\Phi_{\text{MRS}}$  up to 10%. Within the large sequence of metavolcanic rocks there are two fractured zones whereas only the deeper one (48–58 m b.g.s) shows an increase in  $\Phi_{\text{MRS}}$  up to ~4% while no free water was detected at the shallower fractured zone (32–37 m b.g.s.) enriched with clay. The Lameira site represents the lowest water storage capacity as compared to the other four sites evaluated and that is reflected by the low  $H_{\text{wm}} = 0.7$  m estimated for the interval of 0–60 m b.g.s. This value is low even for secondary porosity rocks.

In St-Cyr-en-Val,  $\Phi_{\text{MRS}}$  rapidly increases with depth in the unsaturated zone from 2 to 13% (Fig. 3b) reflecting an unsaturated zone profile sequence of rainwater moisture, capillary fringe and finally a saturated zone below the groundwater table. From the groundwater table level  $\Phi_{\text{MRS}}$  gradually declines, reaching a local minimum at ~23 m b.g.s. slightly above an impermeable dolomite layer at 25–28 m b.g.s. The second, karstic aquifer is well reflected by the gentle increase of  $\Phi_{\text{MRS}}$  up to 5–6% at about 30–42 m b.g.s. which further decreases with depth reaching zero at the level 52–60 m b.g.s. coincident with underlying low permeable sandstone aquitard. The third karstic aquifer is not detected due

to the influence of the overlying conductive layers (Legchenko et al., 1995). St-Cyr-en-Val has  $H_{wm} = 2.9$  m integrated over the 0–60 m depth interval which is typically quite low for the karstic aquifers.

MRS soundings in Botswana in general are difficult to perform not only because of usually low S/N due to the relatively low earth's magnetic field and quite high natural noise (Roy and Lubczynski, 2000b) but also because of the low effective porosities of the Ntane Sandstone target aquifer of approximately 2–6%. In Palla Road, the shallow groundwater table (11.9 m) is well marked by the inflection point of  $\Phi_{MRS}$ . The overlying zone of silty sandstone (11.9–18 m) is substantially saturated by upward leakage showing no  $\Phi_{MRS}$  difference as compared to the underlying aquifer. Below 18 m b.g.s.  $\Phi_{MRS}$  reflects the pattern of the thick Ntane Sandstone aquifer interchanging with coarse, medium and fine lithology sections, which partly can also be influenced by poor S/N ratio, particularly at the deeper sections analyzed. The highest  $\Phi_{MRS} \sim 6\%$  values are observed within the coarse sandstone sections enhanced additionally by the abundant open fractures. In contrast to the Palla Road case, the Serowe case characterizes a 68 m deep, unconfined aquifer.  $\Phi_{MRS}$  shows proper zero water content down to  $\sim 47$  m b.g.s., which further increases with depth up to  $\sim 8\%$  (Fig. 3b) at  $\sim 70$  m b.g.s. within the well sorted coarse sandstone. Interestingly, with different  $\Phi_{MRS}$  (0.08 and 0.06) and different  $S_y$  (0.04 and 0.02) in the Serowe and Palla Road locations, the  $S_r = \Phi_{MRS} - S_y = 0.04$  was obtained for both cases which indicated similar primary porosity but different secondary porosity of the Ntane sandstone aquifer. A similar was also the  $H_{wm}$ , which for Palla Road is 4.5 m and for Serowe 4.2 m, both estimated for the 100 m depth interval. Based on the  $\Phi_{MRS}$  data, it was not possible to precisely estimate the groundwater table level due to the loss of the resolution with depth in the inversion. Considering the MRS measurement accuracy in dual porosity sandstone rocks, it is expected that due to the 30 ms dead time instrumental limitation, a fraction of the fine matrix porosity was undetectable. If the entire pore size spectrum was measured, the  $H_{wm}$  would probably be larger.

The main current limitations related to the interpretation of the  $\Phi_{MRS}$  signal can be listed as follows: (1) lack of exact relation between  $\Phi_{MRS}$  and

$\Phi_f$ ; (2) unavailable separation of signal contributions of water of unconnected and dead-end porosity from overall  $\Phi_{MRS}$  – particularly important in  $n_e$  determination; (3) difficult separation of water signal contribution of  $\theta_f$  from overall  $\Phi_{MRS}$  – particularly important in  $S_y$  determination; (4) problems in interpretation of laterally heterogeneous aquifers (e.g. fractured aquifers) related to the availability of 1D inversion only; (5) equivalence error in interpretation of  $\Phi_{MRS}$ ; (6) distorting influence of electrically conductive layers.

### 3.2. Hydraulic conductivity and transmissivity by decay time constant

There is no doubt about the distinct relationship between the decay time constant ( $T_d$ ) parameter obtained from the signal decay inversion (Figs. 2c and 3c) and the aquifer flow parameters hydraulic conductivity ( $K$ ) or transmissivity ( $T$ ).  $T_d$ , in Eq. (1) indicates how fast the signal decays after excitation which in microscopic scale is understood as the time required by the excited precessing nuclei to make a series of hits against the solid walls of the rock pores to loose energy and phase coherency.  $T_d$  is a measure of how free (how extractable) the water is.

Within NMR technology, three  $T_d$  types are distinguished:  $T_1$  (longitudinal relaxation),  $T_2$  (transverse relaxation) and  $T_2^*$  (free induction decay time constant) as described in Kenyon (1997). In the current standard MRS implementation mainly  $T_2^*$  is evaluated although recently with longer acquisition time,  $T_1$  can also be estimated. The measurement of  $T_2$ , which, unlike  $T_2^*$ , does not include the effect of non-uniformity of the static magnetic field is not yet available in the commercial MRS instrumentation. In the absence of magnetic effects, the MRS-measured  $T_2^* \approx T_2$ .

The first MRS empirical relationship between  $T_2^*$  and rock type dependent pore size was published by Schirov et al. (1991) and later on extended by adding the NMR description of a very short decay rate available in the borehole logging (Allen et al., 1997), see Table 1.

Table 1 shows that  $T_2^*$  decreases towards finer rock materials with smaller pore size. It shows also, that MRS does not measure signals with very short  $T_2^*$  corresponding to very fine pore size.

Table 1  
Empirical NMR relationship relating decay rate with aquifer media, after Schirov et al. (1991), entry in italic is from Allen et al. (1997)

Signal decay rate	Petrophysical information	MRS detectability
$T_2 < 3$ ms	<i>Clay bound water</i>	No
$T_2^* < 30$ ms	Sandy clays	No or marginally
$30 < T_2^* < 60$ ms	Clayey sands, very fine sands	Yes
$60 < T_2^* < 120$ ms	Fine sands	Yes
$120 < T_2^* < 180$ ms	Medium sands	Yes
$180 < T_2^* < 300$ ms	Coarse and gravely sands	Yes
$300 < T_2^* < 600$ ms	Gravel deposits	Yes
$600 < T_2^* < 1500$ ms	Surface water bodies	Yes

Fortunately, the most interesting hydrogeological layers, namely permeable ones, are well measured despite the mentioned limitation.

In the standard MRS signal decay inversion (Fig. 3c), depth dependent distribution of  $T_2^*$  is used to evaluate aquifer permeability with depth and to discriminate layers having the same or similar  $\Phi_{\text{MRS}}$  but different permeability like coarse sand and clayey sand. The  $T_2^*$  inversion is less developed and less reliable than  $\Phi_{\text{MRS}}$  inversion, it loses resolution quicker with depth and is more susceptible to magnetic effects i.e. rock-water magnetic susceptibility contrast or the earth's field inhomogeneity.

In Waalwijk-2 (Fig. 3c), the unsaturated zone is well marked by low  $T_2^*$  values. After passing the break point at 6 m b.g.s. correspondent to the level of the groundwater table,  $T_2^*$  starts to increase. This reflects the change of granulometry from fine through medium to coarse, represented by the layer of gravel at depth interval 14.5–17.5 m b.g.s. Below this,  $T_2^*$  declines within the thick layer of medium sand intercalated by several thin, fine sand layers. This is in good agreement with the  $T_2^*$  description although its continuous decline with depth does not really fit with the occurrence of the coarse material layer at 33–39 m b.g.s. where an increase of  $T_2^*$  would rather be expected. Such disagreement might be either attributed to substantial addition of the fine sand and loam material in that layer at the location of the test or to the fact that already at this depth the  $T_2^*$  inversion is unreliable. An analysis of the deeper section of the  $T_2^*$

suggests that the latter option is more likely because below 52 m b.g.s.,  $T_2^*$  inversion shows rising  $T_2^*$  in the clay layer where obviously the opposite effect is expected. Legchenko et al., (2002) point out general problems of the  $T_2^*$  inversion stating that relaxation time is resolved down to 70–80 m only. Waalwijk-2, characterized by groundwater abundance at the shallow depth, indicates that the depth to which the relaxation time is resolved can be substantially lower.

In Lameira,  $T_2^*$  is not continuous (Fig. 3c) due to the non-permeable hard rock layers present. The first free water detected by MRS at ~3 m b.g.s. in the clay-rich soil is characterized by a short decay time of 30 ms. Another groundwater occurrence in the conglomerate layer is registered by three values with one going up to 400 ms indicating coarse openings containing water. Finally the deepest  $T_2^*$  record of 150 ms at ~54 m b.g.s., corresponds to the permeable fractured metavolcanic layer. As expected the shallower fractured metavolcanic layer sealed with clay was not detected.

In St-Cyr-en-Val (Fig. 3c) shallow alluvial deposits indicate quite high decay time of 150–250 ms further increasing with depth within the sand and gravel layer up to 800 ms. As expected a drop of  $T_2^*$  is observed in the marl confining unit after which  $T_2^*$  starts rising again towards the peak of  $T_2^* > 800$  ms which corresponds to the upper karstic limestone layer. The second limestone layer was not detected.

In Palla Road,  $T_2^*$  pattern is irregular due to poor S/N with typical values around 100 ms. Along the first 6 m within the Kalahari sand,  $T_2^*$  is not determined due to low water content. The leakage zone below (12–18 m b.g.s.), has a decay rate <100 ms correspondent to fine sand as indicated by the borehole information. An aquifer starting at 18 m b.g.s., is marked by an increase of  $T_2^*$  above 100 ms, which further drops with depth to 40 ms at ~25 m b.g.s. reflecting a thin layer of consolidated silty sandstone (35–65 m b.g.s.). Below this,  $T_2^*$  rises again within the well-sorted fine to medium grain, productive sandstone aquifer, containing main water resources.

In the case of Serowe, in the first 40 m of unconsolidated Kalahari sand,  $T_2^*$  is not determined due to low water content. At 40 m b.g.s., perched Kalahari sand water above the top of the Ntane Sandstone layer shows maximum  $T_2^* = 140$  ms, which continues to decrease to 80 ms at 60 m b.g.s.

still within the unsaturated zone. From 60 m b.g.s.,  $T_2^*$  is constant, whereas  $T_2^*$  disturbance would rather be expected due to the groundwater table occurrence at 68 m b.g.s. and the borehole confirmed increase of permeability with depth. This suggests that deep section of  $T_2^*$  is less reliable due to the common MRS problem related to the loss of resolution with depth.

The available quantitative expressions of the relation between  $T_d$  and flow property parameters are only of empirical nature. The most frequently used empirical ‘MRS-to-hydraulic’ relation is Eq. (2) (Seevers 1966), which besides  $T_d$  uses also  $\Phi_{\text{MRS}}$  and proportionality factor ( $C$ ) to determine permeability. Depending on  $C$ , the same formula can also be used to define hydraulic conductivity (Kgotlhang, 2000; Legchenko et al., 2002).

$$K = C \Phi_{\text{MRS}}^a T_d^b \quad (2)$$

$C$  is a formation-specific proportionality factor and therefore it must be re-estimated for each rock type and deposition environment.

As for parameters  $a$  and  $b$ , Seevers (1966) assumes  $a = 1$  and  $b = 2$ , Kenyon et al. (1989) assumes  $a = 4$  and  $b = 2$  while Dunn et al. (1999) studied the correlation between theoretically computed permeability, porosity, formation factor and NMR relaxation times for periodic porous media of identical touching and overlapping spheres. They obtained values of  $b$  in the range of  $1.4 \div 2.0$  while  $a$  was largely variable depending on  $b$ . They finally concluded  $a$  to be less relevant because its large increase can be easily offset by a modest increase in  $b$ . In MRS, Yaramanci et al. (1999) proposed formula  $K = 1.17 T_d^{4.14}$  established for fluvio-glacial deposits investigated in Germany and later generalized to statement  $K \sim T_d^4$  (Yaramanci et al., 2002) where  $T_d$  is given in s and  $K$  in m/s. Application of this formula for the first aquifer at Waalwijk-2 by integrating  $T_d$  over the entire thickness of the aquifer (6–52 m) results in  $K \approx 70$  m/d i.e. a factor  $\sim 3$  higher than the  $K = 24$  m/d indicated by the REGIS model (TNO, 2002).

The parameters  $a$  and  $b$  are different for different rock types like igneous, volcanic, sedimentary and metamorphic rocks because of different hydraulic porosity models like primary porosity, secondary porosity, double porosity and karstic porosity. For

example Kenyon’s approach  $K \sim \Phi_{\text{MRS}}^4 T_d^2$  was particularly suitable in dual porosity sandstone media (Kenyon et al., 1989; Sen et al., 1990) while Seevers formula  $K \sim \Phi_{\text{MRS}}^1 T_d^2$  gave better results in secondary porosity media of diorite, gneiss and karstic porosity of limestone rocks (Legchenko et al., 2002). More research and empirical material is needed to establish generic guidelines for appropriate use of parameters  $a, b$  and  $C$  of Eq. (2) in various rocks with various hydraulic porosity models.

A formation-specific proportionality factor  $C$  in Eq. (2), can be relatively easily established by correlation function when several coincident data points of  $T_d$  (MRS data) and  $K$  or  $T$  (hydrogeological data e.g. from pumping tests and/or numerical models) are available. An example of logarithmic correlation between MRS transmissivity and pumping test transmissivity integrated with depth, is presented by Legchenko et al. (2002) who also present results on the use of  $T_1$  for  $T$  determination.

By applying standard decay analysis as illustrated in Fig. 3c important hydrogeological information can be masked due to the averaging process inherited in the standard NUMIS MRS inversion. This disadvantage can be partially overcome by applying so called multi-decay analysis (Roy, 2000; Mohnke et al., 2001) only possible over data sets with high S/N approximately  $> 60$ . In Fig. 6 an example of multi-decay analysis is illustrated. In Fig. 6a the recorded NMR signal amplitude is displayed as a function of the decay time. A measured NMR signal at the Waalwijk-2 site is illustrated by thick, gray, dashed line. The standard MRS data processing fits a single exponential decay rate to the measured signal. This fit is displayed as ‘MRS inversion model (single  $T_2^*$ )’ line and it is quite good except for the early part ( $< 60$  ms) and the late part ( $< 240$  ms). The measured signal is further analyzed into three exponential components (30, 200 and 800 ms) which are illustrated, respectively, with a thin, medium and thick gray curve. The resultant from these three components is shown by a ‘Resultant fit (30 and 200 and 800 ms)’ curve. In this last case, the fit is considerably better than the single exponential case. Following the strategy used in NMR pore size analysis (Gallegos and Smith, 1988; Kenyon et al., 1989; Howard and Kenyon, 1992), it is assumed that each pore decays as a single exponential and that the pores decay independently of each other.

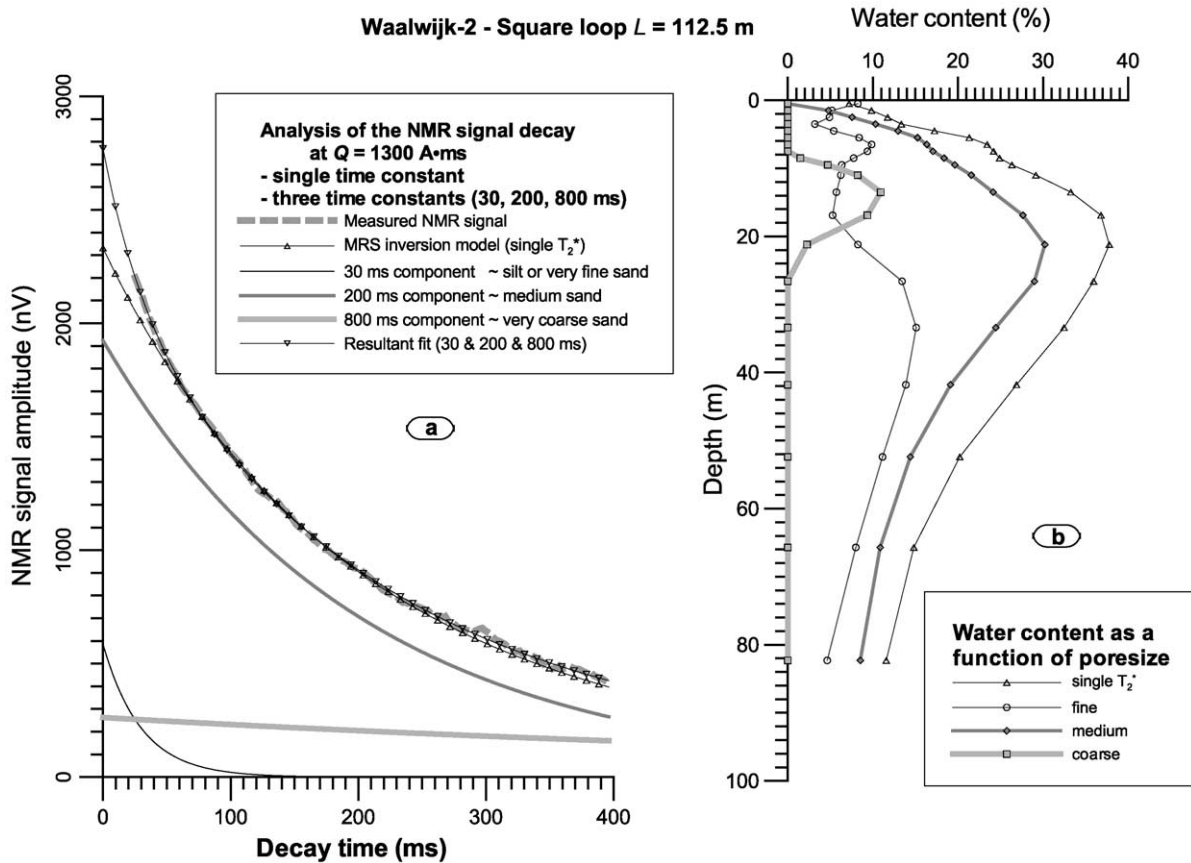


Fig. 6. Multi-decay signal analysis: (a) Waalwijk-2 NMR signal decay for  $Q = 1300$  A.ms analyzed into one and three decay time constants; (b) Corresponding data inversion into 3 pore size classes using complete sounding data set.

An observed decay curve is then analyzed as a sum of single exponential terms, which when properly rescaled correspond to pore-size distribution (Howard and Kenyon, 1992). In that context, MRS provides free water content as a function of depth for a number of pore size classes. This strategy further assumes that the magnetic field is homogeneous and that there is no magnetic susceptibility contrast i.e.  $T_2^* = T_2$  at the scale of the MRS survey. This is a reasonable assumption for many locations in MRS work but it is not normally the case in laboratory or current logging NMR work. Fig. 6b is the conclusion from the exercise illustrated in Fig. 6a where instead of getting a single water content as in the standard inversion [i.e. the 'MRS inversion model (single  $T_2^*$ )' the same as in Fig. 3c], the data set is now inverted into three

pore-size classes (fine, medium and coarse) illustrated with thin, medium and thick curves, respectively. An analysis of these curves (Fig. 6b) indicates, that on the first meter below the surface, at the time of the survey, all the available water was in the fine fraction. From borehole data it is known that the coarsest pore size material occurs within the interval 10–21.5 m b.g.s. This interval coincides with the rise of the coarse water content fraction and the drop of the fine water content fraction (Fig. 6b). This combination is indicative of high hydraulic conductivity with the maximum at  $\sim 14$  m b.g.s. not necessarily coincident with the maximum value of effective porosity at  $\sim 21$  m b.g.s. estimated by the maximum  $\Phi_{\text{MRS}}$  (thinnest line). Thus there is a clear distinction between storage and flow properties. The maximum

effective porosity is reached roughly at the depth where the medium pore-size reaches its maximum. Below 21 m b.g.s., an effective porosity decreases gradually both for its fine and medium pore-size components. As is similarly shown in Fig. 3, one must keep in mind that by applying multi-decay analysis the second aquifer was also not detected.

With respect to the aquifer flow property evaluations, the most demanding is the improvement and verification of the relation between decay inversion results and hydrogeological parameters like aquifer transmissivity and/or hydraulic conductivity. The empirical formulas used differ from one rock type to the other and ignore the pore connectivity aspect. This can be improved by simultaneous use of MRS with electrical methods at sites with hydrogeological parameters available. More MRS tests in various hydrogeological environments applying multi-decay analysis and inversion are needed in order to establish functional relation(s) between MRS output and two main aquifer flow parameters, transmissivity and hydraulic conductivity.

#### 4. Aquifer geometry

As discussed, MRS provides free water content and an estimate of permeability with depth. Therefore it can be used for evaluation of the aquifer geometry i.e. the detection of unconfined groundwater table depth and layer boundaries (tops and bottoms) both called hydrostratigraphic boundaries (Fig. 3) and in the future for evaluation of various 2D and 3D hydrogeological features.

There is no universal and unique recipe to mark the position of the groundwater table using combination of  $\Phi_{\text{MRS}}$  and  $T_d$  yet. By comparison with the field data, it can be observed (Fig. 3) that the groundwater table is usually marked by inflection, bend or break points on either  $\Phi_{\text{MRS}}$  (Palla Road) or on  $T_d$  (St-Cyr-en-Val) or on both of them (Waalwijk). Gev et al. (1996) point out the benefit of using MRS in groundwater table determination giving the example of a densely fractured chalk site in Israel, where MRS results were different from early piezometric measurements but became consistent with the piezometric levels after a one-day stabilization period (a situation similar to Palla Road). They postulated that the

regional groundwater table in fractured rocks could have been even more accurately determined using MRS (HYDROSCOPE used) than by direct borehole measurements arguing that the probability of encountering for example multi-layer joints at a depth corresponding to the regional water level is significantly higher for MRS than for boreholes because MRS covers much larger volumes than the volume related to the pumping test. Our experience in MRS application, at probably less fractured environments in Western Spain (i.e. granite, gneiss), indicated however, that in general, an identification of a groundwater table in a hard rock environment is very difficult. It strongly depends on the S/N ratio influenced by the average quantity of water in the unit rock volume (related to the fracture density), which at the sites tested by us was usually too low to be detected accurately with MRS. Furthermore, the inversion routines are 1D, so that no reliable water table determination can be made in the sparsely fractured cases. With the present MRS technology and good S/N ratio, the phreatic groundwater table can be detected in laterally homogeneous layers with an accuracy of one to a few meters (Gev et al., 1996) depending on the depth and hydrogeological situation. Shallow levels are evaluated with higher accuracy, although with the improvement in technology, the improvement of accuracy can also be expected regarding deeper targets.

The combined analysis of  $\Phi_{\text{MRS}}$  and  $T_d$  with depth (Fig. 3b and c) can be applied for the identification of the layer boundaries (tops and bottoms) in the subsurface. In the Waalwijk-2 sounding example, only the first shallow unconfined aquifer is detected by MRS sounding although the aquifer bottom is determined neither on  $\Phi_{\text{MRS}}$  nor on  $T_d$ . In the Lameira case not only the first shallow aquifer but also the second one extending down to 58 m b.g.s. are well detected. Also two aquifers are detected in the case of St-Cyr-en-Val, while the third starting at 60 m b.g.s. was undetectable. The aquifer boundaries in both sandstone cases, Palla Road and Serowe, were quite well detected despite a low S/N ratio. In all five cases analyzed it is observed that below  $\sim 50$ – $60$  m b.g.s. (threshold dependent not only upon the S/N ratio but also upon loop size, ground conductivity, available range of  $Q$ ) the hydrostratigraphic information becomes less reliable and often unreadable.

An evaluation of aquifer hydrostratigraphy with MRS is currently only an approximate estimate because: (1) uncertainty of data interpretation increases with depth (2) it happens as in the Waalwijk-2 case, that abundance of water in the shallow layers masks the occurrence of the underlying layers; (3) the accuracy of the interpretation due to the current 1D inversion limitation is warranted only when the investigated layers are homogenous and parallel to the surface - the expected 2D and 3D MRS inversion will resolve this problem; (4) MRS inversion involves interpretation equivalence and its severity increases with depth. However, contrary to other classical geophysical methods, there is no ambiguity with respect to free water detection and  $H_w$  evaluation.

Very important in a description of aquifer geometry are the 2D and 3D discrete hydrogeological features. These are the bodies of the local aquifer heterogeneity, which often are comparable with the MRS measurement scale. The 2D features are: plane-shaped permeable hydrogeological features like, open fractures, water bearing faults, dykes etc. plane-shaped impermeable hydrogeological features (barriers) like impermeable dykes, sealed fractures and faults; plane-shaped contacts between permeable and impermeable rocks such as sedimentary or tectonic contacts. The 3D discrete hydrogeological features comparable with the MRS measurement scale are: subsurface features such as tectonic structures, buried channel fills, facies changes and variously shaped karstic bodies and cavities. With present MRS technology due to the 1D limitation, 2D and 3D discrete hydrogeological features are recognized only if their size is comparable with the volume investigated. Such recognition is volumetric, treated as water content percentage compared to the total volume investigated without spatial identification (see below). However, as soon as the 2D and 3D inversions with hardware and field procedure improvements become available, an appropriately designed surveys will yield information not only about storage ( $\Phi_{MRS}$ ) and flow property ( $T_d$ ) with depth but also on location, dimension, and the geometrical shape of the investigated targets provided  $\Phi_{MRS}$  contrast and  $T_d$  contrast will be large enough to be detected against the response of the bulk media. Warsa et al. (2002) have already initiated this type of research.

## 5. Volumetric data integration

The MRS investigation similar to other surface geophysical methods refers to large investigated volumes, usually in a range of several thousand  $m^3$  (up to  $\sim 10^6 m^3$ ) of subsurface media according to the size of the loop and  $Q$  excitation value used. The measured MRS response can be currently interpreted (e.g. overall water content in the measured volume) only if the investigated subsurface is nearly homogenous and isotropic regarding storage and flow property within the scale of each discrete layer assumed to be parallel to the surface. In heterogeneous and anisotropic subsurface, as mentioned, 1D inversion can only provide an estimate averaged over the investigated volumes in layers parallel to the surface.

Information from joint analysis of  $\Phi_{MRS}$  and  $T_d$  with depth (Fig. 3b and c) can therefore be used in the semi-quantitative judgment of the aquifer potential. The unconsolidated rocks are characterized by high  $\Phi_{MRS}$  and high  $T_d$  like the shallow aquifer in the Waalwijk-2 case indicate a water rich aquifer. Low  $\Phi_{MRS}$  and high  $T_d$  are characteristic for karstic aquifers (St-Cyr-en-Val) which might be very productive despite of low  $\Phi_{MRS}$ . Low  $\Phi_{MRS}$  and low to moderate  $T_d$  refer to secondary porosity aquifers (Lameira) while moderate  $\Phi_{MRS}$  and moderate  $T_d$  characterize double porosity aquifers (Palla Road, Serowe). Cases of moderate or even high  $\Phi_{MRS}$  and low  $T_d$ , usually represent clayey or silty semi-permeable aquitards. A combination of low  $\Phi_{MRS}$  and low  $T_d$  usually show impermeable aquiclude. In the vadose zone, low to intermediate  $\Phi_{MRS}$  and variable  $T_d$  are common.

Information obtained from MRS inversion can also be used as input data for groundwater modelling, where one-to-one correspondence between MRS loop position and model grid cell (voxel) is expected. Currently such correspondence works well only in homogenous and isotropic investigated layers parallel to the surface. In heterogeneous and anisotropic layers the signal contribution of the subsurface investigated volume is averaged but not yet well defined. It implies that the accurate, one-to-one correspondence between the MRS loop position and the related model grid cell (voxel) cannot explicitly be made yet. It is expected however that in the near future, depending on the task



realized, MRS method will be able, either to average the volume investigated (as it happens already now) or similar to tomographic brain imaging, to 2D and/or 3D scan the hydrogeological features in the volume investigated. By changing the size of the loop and/or by using multiple detectors like in a current resistivity imaging technique, through the alteration of the excitation value, MRS is likely to be compatible for matching the inversion volume with the hydrogeological target volume (e.g. discretized cell or voxel of the numerical model). Such a unique approach will allow also for a substantial reduction of the scale problem, known in numerical groundwater modelling (Lubczynski, 1997).

## 6. Well siting

At the regional scale, favorable well siting locations like regional hydrogeological structures are often detectable using remote sensing image interpretation and/or airborne geophysics. At the local scale, precise well siting is in most cases successful with standard ground exploration geophysics methods. The disadvantage of such methods is that they cannot provide predictive information about well yields. The MRS method in its current implementation (NUMIS) is not optimized for well siting in laterally heterogeneous conditions. Such a task is often handled by electromagnetic (EM) profiling and/or resistivity profiling methods while MRS provides an estimate of the yield at the site selected. The accuracy of such yield prediction however is constrained by the S/N ratio, the complexity of the water response from different rock types, 1D inversion limitation and insufficient hydrogeological testing and verification. It means that as yet, the yield prediction can only be made in the areas where correlation between the MRS results and borehole data is available. Examples of projects with such area-specific correlations have already been reported from different rock environments. Good correlation between the MRS inversion parameters ( $\Phi_{\text{MRS}}$  and  $T_d$ ) and well abstractions was observed for the Botswana Ntane sandstone aquifer (Kgotlhang, 2000). In fractured diorite of Saudi Arabia, Legchenko et al. (2002) showed the distinct correlation between borehole specific capacities and

estimates of specific capacity derived from MRS. They used a linear relation of MRS calculated transmissivity applying 'Seevers formula' for calculation of hydraulic conductivity. In unconsolidated deposits (sand, silt and clay) in Cambodia, Vouillamoz et al. (2002) proposed MRS as a tool for production well siting. They correlated successfully MRS transmissivity with pumping test transmissivity. Based on a financial analysis, the authors also point out that, currently, the borehole success rate can be substantially improved by joint use of MRS with other geophysical methods like resistivity and electromagnetic surveys. Another type of improvement on the joint MRS inversion supported by vertical electrical sounding is reported by Hertrich and Yaramanci (2002). Such improvements in 2D and 3D MRS scheme and the accumulation of experience over various hydrogeological environments will allow the MRS groundwater exploration and evaluation tasks to be performed with less reliance on the need for area-specific borehole correlation data. With improvement of the S/N ratio, decay time constant (introduction of  $T_1$ ) and incorporation of the phase shift in the inversion algorithm, the reduction of the MRS distortions attributed to e.g. the influence of electrically conductive rocks is expected. The MRS data can then be reliably interpreted at yield prediction tests in an economically sound way.

## 7. Water in unsaturated zone and groundwater recharge

There is no non-invasive method yet capable of providing a quantitative and reliable (as compared to the gravimetric method) description of the water content (moisture) of the unsaturated zone. Electrical and electromagnetic methods, always considered as valuable contributors, play an important role in unsaturated zone investigation but only in a qualitative manner. The relationship between apparent resistivity and water content is more complex in the vadose zone than in the saturated zone. Moreover, the measured resistivities are mostly affected by an increase of conductance when the water particles are electrically interconnected among each other, which is a function of the 'wettability' of the mineral grain-water interface. Ground penetrating radar (GPR) may

supply some shallow information about the localization of sharply defined variations in water content (dielectric changes) in a clean, medium to coarse sand environment. GPR can map the water table accurately although its capability is quickly impaired by the presence of conducting material such as saline water or clay.

As mentioned MRS detects free water content, which combines retained water and gravitational water. Currently with MRS it is not possible to differentiate these two water types. It is however known in hydrology that soil suction pressure at a specific retention capacity ( $S_r$ ) is independent of the soil type and approximately equal to  $-340$  mBar (Dingman, 1994) so the excess of water above  $S_r$  resulting in suction pressure decline is regarded as gravitational water (recharge). This relation can be used in determination of the generic functions for various rock (soil) types and hydrological conditions, correlating MRS measurement of unsaturated capillary retention with profile soil moisture and soil suction pressure measurements, all three being performed in the in situ monitoring mode. Standard soil suction pressure sensors could control such change while the standard soil moisture sensor could provide comparison with the MRS water content all operated by an automatic data acquisition system.

The soil moisture profile and soil suction pressure sensors are already scientifically accepted tools for recharge modelling. However, installation of such sensors is cumbersome (usually from deep excavated shafts), limited to shallow depth and restricted to 1D evaluation. The MRS technology with its surface non-invasive approach and volumetric averaging effect has the potential to overcome these problems. Since the vadose zone is usually relatively shallow a lightweight version of the MRS would suffice, and it could be installed permanently or temporarily in monitoring mode.

## 8. Groundwater salinity

Attempts made in the application of MRS in saline groundwater environments (Goldman et al., 1994; Shushakov, 1996) indicated that MRS is not an appropriate method for groundwater salinity detection

having limitations in performance in conductive environments. We foresee future MRS application in saline groundwater environments rather in combinations with electric/electromagnetic methods, like for example the optimal combination with TDEM (Goldman et al., 1994), combining the strength of MRS (as water quantity estimator) and TDEM (as salinity estimator) in one common loop setup.

## 9. Direct determination of groundwater contamination?

The application of MRS for contamination assessment is still unknown but certainly its detection potential is physically restricted to the contaminants containing hydrogen. To our knowledge, the MRS technology has not yet been tested to detect hydrogen-containing fluids other than water. However such experiments have already been performed under laboratory conditions using the NMR spectroscopy on hydrocarbon contaminants such as gasoline (Hedberg et al., 1993; Daugney et al., 2000).

The laboratory NMR uses as a principle the partitioning of the wide range of different relaxation time constants  $T_1$  to differentiate liquids filling the rock pores. In order to assess the behavior of the water-gasoline mixture, Hedberg et al. (1993) performed a complex test measuring systematically  $T_1$  in varying water and gasoline contents in a sandstone matrix. The experiment indicated that a water-saturated matrix had substantially lower  $T_1$  than a gasoline-saturated matrix. When gasoline coexisted with water in the pore space, the water was a stronger wetting agent so the gasoline–rock interaction decreased making the  $T_1$  difference between water and gasoline (in mixture) even more distinct. In a recent experiment on a silica gel matrix, Daugney et al. (2000) proved however, that such a distinct difference was only valid in the presence of paramagnetic substances, in their case, iron-coating material. The laboratory NMR indicated not only differentiation between water and hydrocarbon but also the possibility of quantification of the hydrated components of the rock matrix. These experiments showed a clear relation between gasoline content and signal amplitude although the exact quantitative assessment under laboratory conditions to differen-

tiate gasoline content from water content in the mixture seemed to be difficult (Hedberg et al., 1993). The laboratory experiments pointed out the complicated nature of the joint dependence of the signal amplitude upon the total quantities of water and hydrocarbon present, their pore scale locations, their bulk relaxation constant and the concentration, location and form of paramagnetic substances in the system (Daugney et al., 2000).

Laboratory NMR allows for a wider range of diagnostic experiments than MRS, which is substantially limited by weaker natural earth magnetic field, and does not allow for high and consistent S/N ratios available in laboratory conditions. It is only recently, that  $T_1$  was implemented in the MRS technology and  $T_2$  is not available as yet. Therefore currently it is still unlikely that trace amounts of hydrated contaminants can be detected with MRS in groundwater.

## 10. Evaluation of transport parameters?

In hydrogeology, transport parameters are in most cases assessed by the tracer tests. Field tracer experiments, although providing data on the pore space, after an inversion of the breakthrough curves, are always limited to the scale of the tracer test. None of the field methods is able to identify spatially (visualize) the framework of the pores, the main factor controlling transport of water. So far such processes have been successfully identified only in laboratory conditions, first in static time series using X-ray computer tomography (Reinken et al., 1995) and recently directly in motion through magnetic resonance imaging (MRI). Greiner et al. (1997) and Oswald et al. (1997) applied clinical MRI and a paramagnetic substance ( $\text{CuSO}_4$ ) as a tracer over the columnar physical model, filled with silica glass beads to acquire 3D tomographic information allowing the identification of the flow regimes and the following transport parameters: pore water velocity, effective porosity, longitudinal dispersion coefficient and longitudinal dispersivity. Baumann et al. (2000) used a similar laboratory set up but with a natural sediment to image in 3D the pore space and to directly measure the molecular diffusion and the flow of water

within a natural porous media. They concluded that, in a similar way, in the near future, the visualization and parameterization of the reactive transport will also be feasible.

Regarding the potential of MRS use in similar imaging applications one has to be aware that both the Larmor frequency and the flow velocities are much higher in the laboratory conditions than in the field MRS where groundwater flows are much slower and the Larmor frequency is tied to the earth's magnetic field. Moreover, MRS field applications, even at test sites well hydrogeologically documented, experience heterogeneity problems, which in laboratory conditions can be well controlled. It seems therefore, that direct flow visualization with MRS will remain out of reach for quite a long time. In a shorter term, however, is foreseen the MRS visualization of porous media in terms of pore-size distribution, namely 3D visualization of water content as a function of discrete pore-size classes showing the spatial structure and texture of subsurface.

## 11. Conclusions

1. MRS is a new and very promising hydrogeophysical method. In contrast to other classical geophysical methods it is water selective, and therefore is much less ambiguous in groundwater assessment.
2. The MRS technique is still undergoing development not only regarding hardware but also data interpretation. There are hydrogeological situations like the Waalwijk-2 water abundant case, where despite a very high and very suitable signal to noise ratio, the method is unable to resolve the data down from 50–60 m b.g.s.
3. In MRS, the measured water content ( $\Phi_{\text{MRS}}$ ) is assumed to be equal to free water content ( $\Phi_f$ ) although the systematic evaluation of the reliability of the accuracy of this statement is not available. If in the saturated aquifer condition the unconnected and dead-end porosity and/or fracturing can be neglected, then  $\Phi_{\text{MRS}} = n_e$ . Specific yield can be derived from  $S_y = \Phi_{\text{MRS}} - S_r$  which slightly underestimates  $S_y$  due to

the current hardware constrained underestimation of total water content disregarding bound water with signal decay  $< 30$  ms. With such limitation and with current assumption of  $\Phi_{\text{MRS}} \cong \Phi_f$ , more correct is the formula  $S_v = \Phi_{\text{MRS}} - \theta_f$ , which however is less practical due to the difficulties in  $\theta_f$  estimate.

4.  $T_d$  is correlated with hydrogeological flow parameters  $K$  and  $T$ . Although this correlation is already expressed by an empirical, media dependent formula linking  $K$  with  $T_d$  and  $\Phi_{\text{MRS}}$ , research is still required on this topic. In field applications this formula has to be calibrated by borehole data for its quantitative use. As an improvement complementary multi-decay analysis is proposed.
5. Aquifer geometry is estimated currently as a 1D task with the resolution decreasing with depth. Shallow groundwater table and shallow layer boundaries in homogenous isotropic sites can be relatively well determined despite the equivalence inherited in the data interpretation increasing with deeper targets. Particularly those deeper than  $\sim 50$  m b.g.s., are less reliably evaluated. Small-scale variability (e.g. heterogeneity in the MRS sounding scale) is not recognizable yet with current MRS technology (1D limitation). With technology improvement this problem will be gradually removed so that MRS will be able to scan target water volumes.
6. The 1D MRS volume-averaging scheme is suitable for quantitative storage parameterization and semi-quantitative flow property parameterization assuming homogeneity and isotropy of the layers parallel to the surface. This is particularly suitable for regional numerical groundwater modelling where similar assumptions are made and where MRS inverted volume can roughly match the model grid. The exact volumetric match will be available as soon as 2D and 3D MRS data acquisition and data inversion become available.
7. Currently, MRS is not optimized yet for well siting in laterally heterogeneous environments so other geophysical profiling techniques may be more efficient in this task. Present MRS inversion parameters however, can already be used to evaluate the suitability (potential productivity) of well sites, but only after calibration by well pumping test data. Joint use of MRS with resistivity and electromagnetic survey and joint inversion can improve borehole success rates in well siting.
8. MRS detects water in an unsaturated zone and therefore it seems there is a good future for MRS applications in monitoring of unsaturated water fluxes. With the current technology, this is still impractical because of present heavy instrument design, having instrumental limitations in the measurement of water decay times shorter than 30 ms (clay, clayey very fine sand) and focused on fairly laborious, deep quantitative groundwater assessment. An alternative could be smaller and cheaper instruments, free from the decay time measurement limitation, which could be used for logger based recharge-evapotranspiration monitoring but also for shallow groundwater exploration.
9. The MRS is not a tool for groundwater salinity determination. However, the integrated use of MRS with electrical and electromagnetic methods increases the reliability of the salinity information.
10. The evaluation of the potential use of MRS in direct detection of groundwater contamination and in tracer imaging, based on the literature study of NMR hydrocarbon detection and tracer imaging in laboratory conditions indicates that the MRS technique similar to NMR applications, is restricted to the substances containing hydrogen and that the implications of the field scale of the MRS experiment and heterogeneity involved make it additionally challenging.
11. So far the MRS method has been known mainly in the geophysical community. This community stimulates technological MRS development. Hydrogeologists are the end users of this technique and therefore cooperation in the knowledge transfer between the geophysical and the hydrogeological community, particularly regarding sites with reliable hydrogeological data available is needed to speed up development and verification of the method. It is hoped that this paper will stimulate establishing such a link between the two mentioned communities.

## Acknowledgements

We acknowledge Prof. Dr A.M.J. Meijerink for his critical text remarks, Dr A. Legchenko and IRIS Instruments for the NUMIS related support, A. Costa for the Lameira borehole data, DWA and Wellfield Consulting Services, both from Botswana for the Serowe and Palla Road borehole data, TNO for Walwijk-2 borehole data and ITC funding schema, in particular Dr E. Kusters, for financial support of the MRS research project. Finally we acknowledge Editor-in-Chief and anonymous peer reviewers for their constructive remarks.

## References

- Allen, D., Andreani, M., Badry, R., Flaum, C., Gossenberg, P., Horkowitz, J., Singer, J., White, J., 1997. How to use borehole NMR. Schlumberger's Oilfield Review summer, 34–57.
- Baumann, T., Petsch, R., Niessner, R., 2000. Direct 3-D measurement of the flow velocity in porous media using magnetic resonance tomography. *Environmental Science and Technology* 34, 19.
- Coates, G.R., Marschall, D., Mardon, D., Galford, J., 1998. A new characterization of bulk-volume irreducible using magnetic resonance. *The Log Analyst* 39 (1), 51–63.
- Daugney, C.J., Bryar, T.R., Knight, R.J., 2000. Detecting sorbed hydrocarbons in a porous medium using proton nuclear magnetic resonance. *Environmental Science and Technology* 34 (2).
- Dingman, S.L., 1994. *Physical Hydrology*, Macmillan Publishing Company.
- Dunn, K.J., La Torraca, G.A., Bergman, D.J., 1999. Permeability relation with other petrophysical parameters for periodic porous media. *Geophysics* 64 (2), 470–478.
- Fetter, C.W., 1994. *Applied Hydrogeology*, Prentice Hall, New Jersey, 07458.
- Gallegos, D.P., Smith, D.M., 1988. A NMR technique for the analysis of pore structure: determination of continuous pore-size distributions. *Journal Colloid Interface Science* 122, 143–153.
- Gev, I., Goldman, M., Rabinovich, B., Rabinovich, M., Issar, A., 1996. Detection of the water level in fractured phreatic aquifers using nuclear magnetic resonance (NMR) geophysical measurements. *Journal of Applied Geophysics* 34, 277–282.
- Goldman, M., Rabinovich, B., Rabinovich, M., Gilad, D., Gev, I., Schirov, M., 1994. Application of the integrated NMR-TDEM method in groundwater exploration in Israel. *Journal of Applied Geophysics* 31, 27–52.
- Grabowska-Olszewska, B., Siergiejew, J.M., 1977. Gruntoznawstwo. Wydawnictwa Geologiczne-Warszawa (in Polish).
- Greiner, A., Schreiber, W., Brix, G., Kinzelbach, W., 1997. Magnetic resonance imaging of paramagnetic tracers in porous media: quantification of flow and transport parameters. *Water Resources Research* 33 (6), 1461–1473.
- Hedberg, S.A., Knight, R.J., MacKay, A.L., Whittall, K.P., 1993. The use of nuclear magnetic resonance for studying and detecting hydrocarbon contaminants in porous rocks. *Water Resources Research* 29 (4), 1163–1170.
- Hertrich, M., Yaramanci, U., 2002. Joint inversion of surface nuclear magnetic resonance and vertical electric soundings. *Journal of Applied Geophysics* 50, 179–191.
- Howard, J.T., Kenyon, W.E., 1992. Determination of poresize distribution in sedimentary rocks by proton nuclear magnetic resonance. *Marine and Petroleum Geology* 9, 139–145.
- IRIS Instruments, 2002. [www.iris-instruments.fr/](http://www.iris-instruments.fr/).
- Kenyon, W.E., Howard, J.J., Sezginer, A., Straley, C., Matteson, A., Horkowitz, K., Ehrlich, R., 1989. Pore-size distribution and NMR in microporous cherty sandstones. SPWLA 13th Annual Logging Symposium, Paper LL.
- Kenyon, W.E., 1997. Petrophysical principles of application of NMR logging. *The Log Analyst* March–April, 21–43.
- Kgotlhang, L., 2000. Evaluation of the magnetic resonance sounding technique as a tool for groundwater exploration. Case study—Botswana. Msc thesis. Library of ITC ([www.itc.nl](http://www.itc.nl)).
- Legchenko, A.V., Shushakov, O.A., Perrin, J.A., Portselan, A.A., 1995. Noninvasive NMR study of subsurface aquifers in France. Annual Meeting SEG Houston.
- Legchenko, A.V., Shushakov, O.A., 1998. Inversion of Surface NMR data. *Geophysics* 63, 75–84.
- Legchenko, A.V., Baltassat, J.M., Beauce, A., Makki, M.A., Al-Gaydi, B.A., 1998. Application of the surface proton magnetic resonance method for the detection of fractured granite aquifers. Proceedings of the IV Meeting of the Environmental and Engineering Geophysical Society, September 14–17, 1998, Barcelona, pp. 163–166.
- Legchenko, A., Baltassat, J.M., Beauce, A., Bernard, J., 2002. Nuclear magnetic resonance as a geophysical tool for hydrogeologists. *Journal of Applied Geophysics* 50, 21–46.
- Lieblich, D.A., Legchenko, A., Haeni, F.P., Portselan, A., 1994. Surface nuclear magnetic resonance experiments to detect subsurface water at Haddam Meadows, Connecticut. Proceedings of the Symposium on the Application of Geophysics to Engineering and Environmental Problems. March 27–31, 1994, Boston Massachusetts (USA) 2, 717–736.
- Lubczynski, M.W., 1997. Application of numerical flow modelling combined with remote sensing and GIS techniques for the quantification of regional groundwater resources in hard rock terrains. IAHS Publication No. 241.
- Lubczynski, M.W., Roy, J., 2004. Magnetic resonance sounding (MRS) – new method for groundwater assessment. *Ground Water* 42.
- Maidment, D.R., 1993. *Handbook of Hydrology*, McGraw-Hill, New York.
- Marsily, G., 1986. *Quantitative Hydrogeology*, Academic Press, New York.
- Mohnke, O., Braun, M., Yaramanci, U., 2001. Inversion of decay time spectra from surface-NMR data. Proceedings of Seventh Meeting of Environmental and Engineering Geophysics, Birmingham, Great Britain.
- Oswald, S., Kinzelbach, W., Greiner, A., Brix, G., 1997. Observation of flow and transport processes in artificial porous

- media via magnetic resonance imaging in three dimensions. *Geoderma* 80, 417–429.
- Polubarinova-Kochina, P.Y., 1962. *Theory of Groundwater Movement*. (Translated from Russian by R.J.M. De Wiest), Princeton University Press, Princeton, NJ.
- Rawls, W.J., Brakensiek, D.L., 1985. Prediction of soil water properties for Hydrologic modelling. *Watershed management in the eighties*. ASCE, 293–299.
- Reinken, G., Fuehr, F., Zadgorsky, N., Halling, H., Schult, O., 1995. *BCPC Monogr* 62, 39–44.
- Roy, J., Costa, A.M., Lubczynski, M.W., Owuor, C., 1998. Tests of the SGW-NMR technique within two aquifer characterization projects in the Iberian Peninsula. *Proceedings of the IV EEGS-ES Meeting, September 14–17 1998, Barcelona*, pp. 177–180.
- Roy, J., 2000. MRS surveys under favorable conditions of S/N ratio. *Proceedings of the Sixth Meeting of EEGS-ES, September 3–7, 2000, Bochum, Germany*, P-EM-08.
- Roy, J., Lubczynski, M.W., 2000a. MRS: introduction to a new geophysical technique and its current status; *Iero Congreso Cubano de Geofísica, Memorias de Geoinfo (Proceedings on CD-ROM)*.
- Roy, J., Lubczynski, M.W., 2000b. The MRS technique for groundwater resources evaluation – test results from selected sites in Southern Africa, *Proceedings of the XXX IAH Congress in Capetown/South Africa/26 November–1 December, Balkema, Rotterdam/Brookfield*.
- Roy, J., Lubczynski, M.W., 2003. The MRS technique and its use for groundwater investigations. *Hydrogeology Journal* 11(4), 455–465.
- Schirov, M., Legchenko, A., Creer, G., 1991. A new direct non-invasive groundwater detection technology for Australia. *Exploration Geophysics* 22, 333–338.
- Seevers, D.O., 1966. A nuclear magnetic method for determining the permeability of sandstones. Paper L in *Annual Logging Symposium Transactions*. Society of Professional Well Log Analysts.
- Semenov, A.G., 1987. NMR HYDROSCOPE for water prospecting. *Proceedings of the seminar on Geotomography, Indian Geophysical Union, Hyderabad*, 66–67.
- Sen, P.N., Straley, C., Kenyon, W.E., Whittingham, M.S., 1990. Surface-to-volume ratio, charge density, nuclear magnetic relaxation and permeability in clay bearing sandstones. *Geophysics* 55 (1), 61–69.
- Shushakov, O.A., 1996. Groundwater NMR in conductive water. *Geophysics* 61 (4), 998–1006.
- Timur, A., 1969. Pulsed nuclear magnetic resonance studies of porosity, moveable fluid and permeability of sandstone. *Journal of Petroleum Technology* 21 (6), 775–786.
- TNO, 2002. DINO and REGIS digital data systems at <http://www.nitg.tno.nl/eng/>.
- Todd, K.D., 1959. *Groundwater Hydrology*, Wiley, New York.
- Trushkin, D.V., Shushakov, O.A., Legchenko, A.V., 1994. The potential of a noise-reducing antenna for surface NMR groundwater surveys in the earth's magnetic field. *Geophysical Prospecting* 42, 855–862.
- Trushkin, D.V., Shushakov, O.A., Legchenko, A.V., 1995. Surface NMR applied to an electroconductive medium. *Geophysical prospecting* 43, 623–633.
- Vouillamoz, J.M., Descloitres, M., Bernard, J., Fourcassier, P., Romagny, L., 2002. Application of integrated SNMR-resistivity methods for borehole implementation. A case study in Cambodia. *Journal of Applied Geophysics* 50, 67–81.
- Warsa, W., Mohnke, O., Yaramanci, U., 2002. 3D modelling of surface NMR amplitudes and decay times. *Third ICWRER, Dresden, 22–25 July 2002*.
- WCS (Wellfield Consulting Services), 1994. *Palla Road Groundwater Resources Investigation*, Ministry of Water Affairs of Botswana.
- WCS (Wellfield Consulting Services), 2000. *Serowe Groundwater Resources Investigation*, Ministry of Water Affairs of Botswana.
- Yaramanci, U., Lange, G., Knödel, K., 1999. Surface NMR within a geophysical study of an aquifer at Haldensleben (Germany). *Geophysical Prospecting* 47, 923–943.
- Yaramanci, U., Lange, G., Hertrich, M., 2002. Aquifer characterization using Surface NMR jointly with other geophysical techniques at the Nauen/Berlin test site. *Journal of Applied Geophysics* 50, 47–65.